Acta Pharmaceutica Sinica B 2022;12(2):787−800

Chinese Pharmaceutical Association
Institute of Materia Medica, Chinese Academy of Medical Sciences

Acta Pharmaceutica Sinica B

www.elsevier.com/locate/apsb
www.sciencedirect.com

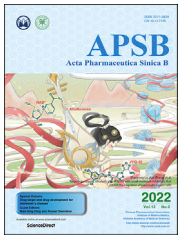

ORIGINAL ARTICLE

TGR5 deficiency activates antitumor immunity in non-small cell lung cancer *via* restraining M2 macrophage polarization

Lifang Zhao[†], Hongyan Zhang[†], Xueqing Liu[†], Shan Xue, Dongfang Chen, Jing Zou[*], Handong Jiang[*]

Department of Respiratory and Critical Care Medicine, Ren Ji Hospital, School of Medicine, Shanghai Jiao Tong University, Shanghai 200127, China

Received 4 March 2021; received in revised form 12 May 2021; accepted 18 May 2021

KEY WORDS

TGR5;
Bile acids;
Tumor-associated macrophages (TAMs);
Tumor microenvironment (TME);
Non-small cell lung cancer (NSCLC);
Antitumor immunity;
Immunotherapy;
cAMP−STAT3/STAT6

Abstract The bile acid-responsive G-protein-coupled receptor TGR5 is expressed in monocytes and macrophages, and plays a critical role in regulating inflammatory response. Our previous work has shown its role in promoting the progression of non-small cell lung cancer (NSCLC), yet the mechanism remains unclear. Here, using *Tgr5*-knockout mice, we show that TGR5 is required for M2 polarization of tumor-associated macrophages (TAMs) and suppresses antitumor immunity in NSCLC *via* involving TAMs-mediated $CD8^+$ T cell suppression. Mechanistically, we demonstrate that TGR5 promotes TAMs into protumorigenic M2-like phenotypes *via* activating cAMP-STAT3/STAT6 signaling. Induction of cAMP production restores M2-like phenotypes in TGR5-deficient macrophages. In NSCLC tissues from human patients, the expression of TGR5 is associated with the infiltration of TAMs. The co-expression of TGR5 and high TAMs infiltration are associated with the prognosis and overall survival of NSCLC patients. Together, this study provides molecular mechanisms for the protumor function of TGR5 in NSCLC, highlighting its potential as a target for TAMs-centric immunotherapy in NSCLC.

Abbreviations: BMDMs, bone marrow-derived macrophages; CM, conditioned medium; LLC, Lewis lung carcinoma; NSCLC, non-small cell lung cancer; SD, standard deviation; TAMs, Tumor-associated macrophages; TME, tumor microenvironment; WT, wildtype.

*Corresponding authors. Tel.: +86 21 68385507; fax: +86 21 58394262.
E-mail addresses: drzouj@163.com (Jing Zou), jianghd@163.com (Handong Jiang).
[†]These authors made equal contributions to this work.

Peer review under responsibility of Chinese Pharmaceutical Association and Institute of Materia Medica, Chinese Academy of Medical Sciences.

https://doi.org/10.1016/j.apsb.2021.07.011

1. Introduction

Non-small cell lung cancer (NSCLC), which accounts for 85% of all lung cancers, continues to be the cardinal cause of fatal malignancies despite recent advances in diagnosis and treatment[1−3]. In recent years, the tumor microenvironment (TME) has emerged as an important role in tumor development and has become a new direction for cancer treatment[4]. Tumor-associated macrophages (TAMs) are found abundantly and considered to be pivotal components of immunosuppressive cells in the TME[5]. TAMs activation is complex and exhibits different phenotypes in tumor process[6]. Generally, macrophages at early stages of tumor initiation show a M1 phenotype which exert anti-tumor activities[7], while pro-tumorigenic TAMs are educated by tumor cells to acquire an immunosuppressive phenotype to promote tumor growth, *via* secretion of multiple anti-inflammatory factors or directly inhibiting the cytotoxic function of $CD8^+$ T cells, and thereby lead to the evasion of immune surveillance[8]. Therefore, TAMs are considered an attractive target for therapeutic intervention with their plastic pro-tumorigenic and anti-tumorigenic functions[9]. Various preclinical studies have demonstrated that inhibiting the recruitment of macrophages or reprogramming their phenotype to limit M2 polarization can inhibit tumor development and improve treatment response[10−13]. High infiltration of M2-polarized macrophages in the primary tumor indicates unfavorable prognosis in NSCLC patients[14]. Therefore, reversing the M2 polarization of TAMs in tumors could be considered a potential therapeutic strategy, and identification of novel molecules able to interfere with macrophage may reveal new targets for TAM-centric anti-tumor immunotherapy.

TGR5 (also known as *GPBAR1*), a cell membrane G protein-coupled receptor specific to bile acid, has an important role in bile acids synthesis, glucose metabolism and energy homeostasis[15]. TGR5 is expressed in macrophages and TGR5 agonist attenuates inflammation factor release in atherosclerosis[16], experimental autoimmune encephalomyelitis[17] and inflammatory bowel diseases[18,19]. Besides, TGR5 activation in macrophages co-cultured with $CD4^+$ T cells inhibited Th1 and Th17 polarization in Vogt-Koyanagi-Harada disease[20]. All these indicated that TGR5 in macrophage plays a role in regulating inflammatory response. Accumulating evidence indicated the potential role of TGR5 in cancer, either in a tumor promoting[21,22] or tumor suppressive fashion[23], as dependent on the biological context and tissue lineage. Our previous study showed that overexpression of TGR5 promoted NSCLC cell proliferation and tumor growth, and was positively correlated with an advanced clinical stage in NSCLC patients. Interestingly, we also observed that TGR5 was expressed in TAMs in NSCLC tissues[24], indicating its potential role in TAMs-associated TME regulation in NSCLC. We thus hypothesize TGR5 promote tumor growth in NSCLC *via* reprogramming TAMs.

In the present study, we aimed to investigate the mechanisms of TGR5 in promoting NSCLC progression. Using *Tgr5*-knockout mice, we discover that TGR5 is required for M2 polarization of TAMs and suppresses antitumor immunity in NSCLC. Our results provide new evidence highlighting the role of TGR5 in the microenvironment in NSCLC.

2. Material and methods

2.1. Patients and tissue samples

Two hundred primary NSCLC tissues, along with the available clinicpathological information and survival statistics, were collected from the Department of Pathology in Ren Ji hospital, School of Medicine, Shanghai Jiao Tong University (Shanghai, China). All included patients signed informed consent forms, and all related procedures were performed with approval from the Ethical Review Boards of Ren Ji Hospital. Correlations between TGR5 and TAM infiltration ($CD68^+$) or M2-like TAMs ($CD206^+$ TAMs) were analyzed in 1032 patients online (https://www.cbioportal.org) using The Cancer Genome Atlas (TCGA, Pan-Cancer Atlas) database.

2.2. Mice and tumor models

Wildtype (WT) and TGR5 knockout ($Tgr5^{-/-}$) mice on a C57BL/6J background were generated and obtained from Bioray Laboratories (Shanghai, China). Animal studies were approved and conducted following the guidelines of the Experimental Animal Ethics Committee of Shanghai Jiao Tong University (Shanghai, China). For subcutaneous tumor models, Lewis lung carcinoma (LLC) cells were subcutaneously injected into the right flanks of WT and $Tgr5^{-/-}$ mice (female, 6−8 weeks). $Tgr5^{-/-}$ mice were identified by PCR analysis of genomic DNA from tail snips and confirmed by using the primers 5′-GATAATGTGCTGTCCC-CACC-3′ and 5′-AGCTGACCCAGGTGAGGAAC-3′. Tumor growth curves were recorded every three days. At the termination of the experiment, tumor tissues were isolated for further experiments. For the experiment with bone marrow-derived macrophages (BMDMs), C57BL/6J mice were depleted of macrophages by intraperitoneal injection of clodronate liposomes (200 μL/mouse; YEASEN, Shanghai, China) 48 h prior to inoculations. All macrophage-depleted C57BL/6J mice were then injected subcutaneously with a mixture of LLC cells plus macrophages derived from WT or $Tgr5^{-/-}$ mice. After implantation, the diameter of the tumors was recorded. Mice were sacrificed at the end of the experiments and tumor-infiltrating lymphocytes were analyzed as described in our previous study[25]. The antibodies used for flow cytometry are described in Supporting Information Table S1.

2.3. Reagents, primers and antibodies

TGR5 antagonist SBI 115 was purchased from MedChemExpress (Monmouth Junction, NJ, USA) and forskolin (adenylate cyclase activator to increase cAMP) was purchased from Selleck Chemicals (Houston, TX, USA). All antibodies used are listed in Table S1 and specific primer sequences are listed in Supporting Information Table S2. cAMP and IL-10 were detected with the cAMP Parameter Assay Kit and Mouse IL-10 Quantikine ELISA Kit (R&D Systems, Minneapolis, MN, USA).

2.4. Cell lines and tumor conditioned medium preparation

The NSCLC cell lines H1299, HCC4006, A549, PC-9, and LLC, as well as the human monocyte cell lines U937 and THP-1 were obtained from the American Type Culture Collection (Maryland, USA) and cultured according to the instructions provided by the manufacturer. All cell lines were authenticated based on STR fingerprinting and used within 20−30 passages. Human U937 cells and THP-1 were differentiated into macrophages by treatment with PMA (200 nmol/L, Sigma−Aldrich, Taufkirchen, Germany) for 48 h. Cancer cell lines were cultured in complete medium, and the medium was replaced by serum-free medium when cell density reached about 80%. After 24 h, new conditioned medium (CM) was harvested, centrifuged in 500×*g* for 5 min, filtrated by 0.22 μm filters, and restored at −80 °C.

2.5. Mouse primary cells extraction and stimulation

Bone marrow cells from WT and *Tgr5*$^{-/-}$ female mice were prepared as described previously[26] and cultured in Iscove's modified Dulbecco's medium (Gibco, Grand Island, NY, USA) containing 10% FBS and 50 ng/mL M-CSF (PeproTech, NJ, USA) for 7 days to obtain BMDMs. To induce M2 differentiated macrophages, BMDMs were cultured with IL4/IL13 (20 ng/mL, PeproTech) for 48 h. To obtain TAMs, tumor CM was added into cultured medium in 1/2 volume for 48 h.

2.6. Immunohistochemical (IHC) staining and analysis

IHC staining was performed as previously described[24]. The antibodies used are listed in Table S1. Five representative fields from each section were assessed by two experienced pathologists. The final IHC score of TGR5 was obtained by multiplying the intensity and percentage scores. To analyze the number of TAMs, CD68-positive cells in tumor regions were counted manually and expressed as cells per field. Positively stained cells that were smaller than the size of circulating T cells (10 μm) were excluded from counting. The expression levels of TGR5 were classified for statistical analysis as follows: < 6, low expression; ≥ 6, high expression. The number of CD68-positive cells in lung tissue was defined as low (< 80 per field) or high (≥ 80 per field).

2.7. In vitro phagocytosis assays

For the phagocytosis assay, different phenotype macrophages were plated into low-attachment 96-wells plates and then co-culture with CFSE-labelled LLC cells. After 2 h, all cells were collected and stained on ice for 30 min with F4/80, then analyzed by flow cytometry. Phagocytosis efficiency was determined as the percentage of F4/80^{+} cells containing CFSE-derived fluorescence.

2.8. Tumor cell proliferation and migration assay

LLC cells were plated onto a 96-wells plate with 2×10^3 cells/well. After overnight starvation and incubation with different CM from BMDMs for indicated time, cell proliferation was quantified by using the sulforhodamine B assay. The cell migration assay was performed in a Transwell Boyden chamber (Corning Costar, USA). LLC cells (2×10^5 cells/well) were seeded into the top chamber, and the bottom chamber was filled with different polarized macrophages. After 12 h incubation, the inserts were stained with crystal violet, and the unmigrated cells were removed. The invasion assay was performed similarly to the migration assay, except the top chambers were coated with Matrigel (BD Bioscience, Franklin, NJ, USA). Images were obtained using an OLYMPUS (Japan) inverted microscope at 200 × magnification.

2.9. CD8^{+} T cell suppression assay

Mouse CD8^{+} T cells were isolated from C57BL/6J mice using a mouse CD8^{+} T cell isolation kit (Stem Cell Technologies, Vancouver, Canada). Then, CD8^{+} T cells were stimulated with αCD3/αCD28 and IL-2 (PeproTech) and cocultured with different phenotype macrophages for 72 h, CD8^{+} T cells were treated with eBioscience™ Cell Stimulation Cocktail (Invitrogen, Carlsbad, CA, USA) for 4 h and then collected and analyzed for CD8^{+} T cell proliferation and functional marker expression by flow cytometry.

2.10. Statistical analysis

The statistical significance of the differences was tested using analysis of variance (ANOVA) or Student's *t*-tests. Survival data were analyzed by the Kaplan−Meier method (log-rank test). Correlational analysis was conducted using chi-square test. A *P*-value less than 0.05 was regarded as statistically significant. All statistical analyses were performed in SPSS v17.0 (IBM, USA) and GraphPad Software (La Jolla, CA, USA).

3. Results

3.1. TGR5 deficiency in mice suppresses LLC tumor growth and the polarization of TAMs to M2-like phenotype

To investigate the role of TGR5 in the tumor microenvironment, LLC cells were subcutaneously inoculated in WT and *Tgr5*-deficient mice in parallel. Genotype of mice were confirmed by PCR analysis and TGR5 was markedly lower in the primary BMDMs of *Tgr5*$^{-/-}$ mice (Supporting Information Fig. S1A and S1B). We found that LLC tumor growth in *Tgr5*$^{-/-}$ mice was significantly slower than those in WT mice (Fig. 1A and B). We then examined the immune cell infiltration in LLC tumors. Compared to the tumors from WT mice, those from *Tgr5*$^{-/-}$ mice exhibited a decreased TAMs infiltration, while the frequencies of total hematopoietic cells, including CD11b, DC, CD3e, CD4^{+} T and CD8^{+} T cells, showed no difference (Fig. 1C and D). Further analysis revealed that TGR5 deficiency caused a decrease in CD206^{+} TAM cells (Fig. 1E), but an increase in M1/M2 ratio and IFN-γ^{+}CD8^{+} T cells frequency as compared to LLC-WT mice (Fig. 1F and G), indicative of the attenuation of M2-like immunosuppressive phenotype of TAMs in *Tgr5*$^{-/-}$ mice. We also found the ratio of monocytes in blood declined in *Tgr5*$^{-/-}$ mice, but the difference was not significant (Fig. S1C). Moreover, *Tgr5*$^{-/-}$ mice showed a decreased level of IL-10 in blood serum (Fig. S1D), but the inflammatory factors such as IL-6, TNF-α and IFN-γ were not obviously changed (data not shown). These results suggest that the restrained polarization of TAMs to M2-like phenotype may contribute to the inhibition of tumor growth in *Tgr5*$^{-/-}$ mice.

3.2. TGR5 deficiency in macrophages restrains the polarization to M2-like phenotypes

We next confirmed the impact of TGR5 deficiency on macrophage *in vitro*. Firstly, BMDMs from *Tgr5*$^{-/-}$ mice (*Tgr5*$^{-/-}$ BMDMs) or WT mice (WT-BMDMs) were stimulated with IL-4 and IL-13. As compared with the WT-BMDMs, we found that *ARG-1* and *IL-10*, the classical M2 markers, were obviously reduced in *Tgr5*$^{-/-}$ BMDMs. Consistent with this result, the proportion of CD206^{+} M2 macrophages was reduced in *Tgr5*$^{-/-}$ BMDMs (Fig. 2A and B). These results indicate that TGR5 was indispensable for M2 polarization of macrophage. To better reflect the impact of TGR5 in the tumor microenvironment, WT-BMDMs were cultured with CM collected from LLC cell culture (LLC-CM), which resulted in an induction of TGR5 expression at both mRNA and protein levels in TAMs (Fig. 2C). Similar results were obtained using CM from

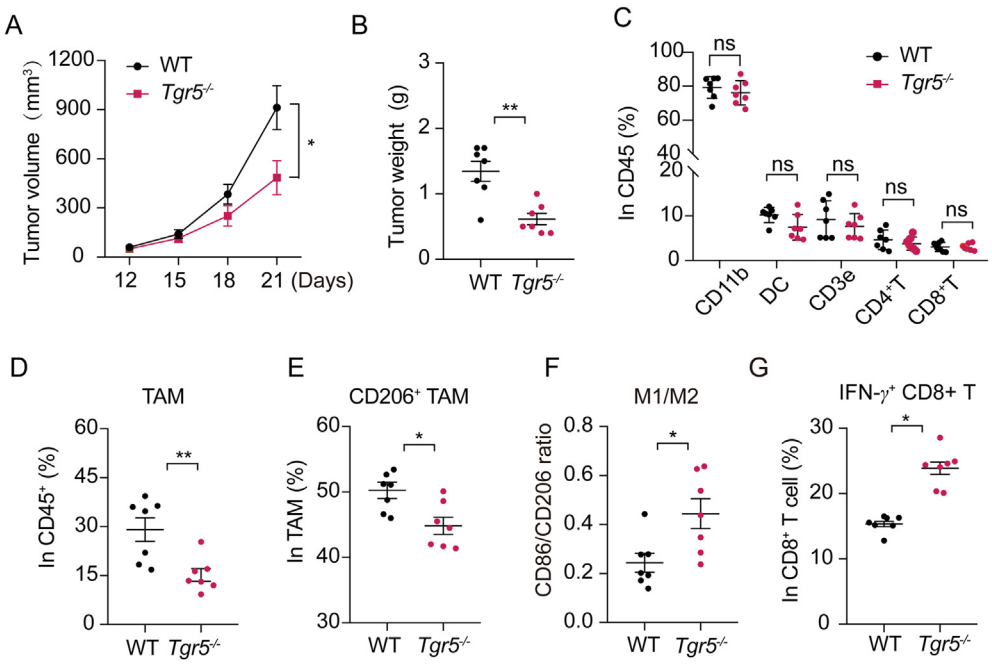

Figure 1 TGR5 deficiency in mice suppresses LLC tumor growth and the polarization of TAMs to M2-like phenotype. Eight-week-old female wildtype (WT) ($n = 7$) and TGR5 knockout ($Tgr5^{-/-}$) ($n = 7$) mice were subcutaneously implanted with LLC cells of 2×10^6 ($n = 7$). Mice were sacrificed 21 days later. (A) Tumor growth curve. (B) Tumor weights. (C)−(G) Flow cytometric analysis of immune subsets in the tumor. The infiltration of (C) $CD11b^+$, DC, CD3e, $CD4^+$ T cells and $CD8^+$ T cells and (D) TAMs ($CD11b^+$ $F4/80^+$) were fluorescent stained and analyzed by flow cytometry. Expression of (E) M2-like TAMs ($CD11b^+$ $F4/80^+$ $CD206^+$), (F) M1 ($CD11b^+$ $F4/80^+$ $CD86^+$)/M2 ratio and (G) IFN-γ^+ $CD8^+$ T cells were determined by flow cytometry. Data are represented as mean ± standard error of mean (SEM). *P* values were determined by two-tailed Student's *t* test, respectively. $^*P < 0.05$, $^{**}P < 0.01$; ns, not significant, compared with the WT group.

different human tumor cell culture (Fig. 2D). Further, we compared the phenotypes of BMDMs from WT and $Tgr5^{-/-}$ mice. $Tgr5^{-/-}$ BMDMs cultured with LLC-CM exhibited a significantly increased M1-related genes expression (Fig. 2E) and suppressed M2-related genes expression (Fig. 2F) compared with the counterpart from WT mice. Flow cytometric analysis further confirmed that $Tgr5^{-/-}$ macrophages presented a reduced of M2 polarization, as indicated by the increased CD86 expression and the decreased CD206 expression (Fig. 2G and H). Meanwhile, we also examined the impact of TGR5 deficiency on macrophage differentiation. TGR5 appeared not required for macrophage differentiation, as the percent of F4/80-positive matured macrophage induced from bone marrow hematopoietic stem cells and bone marrow Ly6C-positive macrophage precursor cells barely changed in *Tgr5*-deficient mice compared with those from the WT control mice (Fig. S1E and S1F). The proliferation of BMDMs also showed no difference between $Tgr5^{-/-}$ and WT groups (Fig. S1G).

To explore whether TGR5 plays a similar role in human macrophages, TGR5 expression in human U937 cells was depleted using siRNAs (Supporting Information Fig. S2A) followed by stimulation with CM from A549 and H1299. As expected, the expression of M1 markers were upregulated in TGR5-silenced U937 cells (Fig. S2B and S2C), yet *IL-10* and *ARG-1*, markers of human M2-like macrophage, decreased significantly in the TGR5 interference group (Fig. S2D and S2E). Consistently, TGR5-overexpressing THP-1 impaired CM-induced M1 polarization but increased M2 mark expression (Fig. S2F−S2J). These results substantiate an important role of TGR5 in promoting M2 polarization of TAMs.

3.3. TGR5 deficiency enhances macrophage phagocytosis and decreases tumor-promoting properties

Macrophages can directly phagocytose tumor cells and acquire a phenotype that displays cytotoxic properties. However, TAMs act as "protumoral macrophages" that largely contribute to promote tumor cell survival, proliferation, and dissemination in TME. We next assessed whether TGR5 could affect phagocytosis of macrophages for tumor cells. CFSE-labeled LLC cells were co-cultured with WT- or $Tgr5^{-/-}$ BMDMs, respectively. M2 macrophage from $Tgr5^{-/-}$ mice exhibited increased phagocytosis of LLC cells compared with those from the WT mice (Fig. 3A). Similar results were also observed in LLC-CM-treated BMDMs. $Tgr5^{-/-}$ BMDMs exposed to LLC-CM showed an increased phagocytosis of macrophages compared from WT-BMDMs, from 3.72% to 8.53% (Fig. 3B). We next examined the effect of TGR5 on macrophage-mediated tumor cell proliferation and migration. CM from WT macrophage increased the proliferation of LLC cells, while the proliferation ability of LLC cells treated with CM from $Tgr5^{-/-}$ macrophage was decreased compared with that of WT-BMDMs (Fig. 3C and D). We also investigated the effects of TGR5 on the migration and invasion of LLC cells. As shown in Fig. 3E and F, the presence of M2 macrophages and CM-treated macrophages obviously stimulated the migration of co-cultured LLC cells. However, $Tgr5^{-/-}$ BMDMs blocked lung tumor cell migration and invasion. Similarly, TGR5-silenced U937 cells showed attenuated effects on the promotion of H1299 cell migration, while TGR5 overexpressed THP-1 cells promoted significant cancer cell migration (Fig. S2K and S2L). Taken together, these results indicate that $Tgr5^{-/-}$ macrophage exhibited

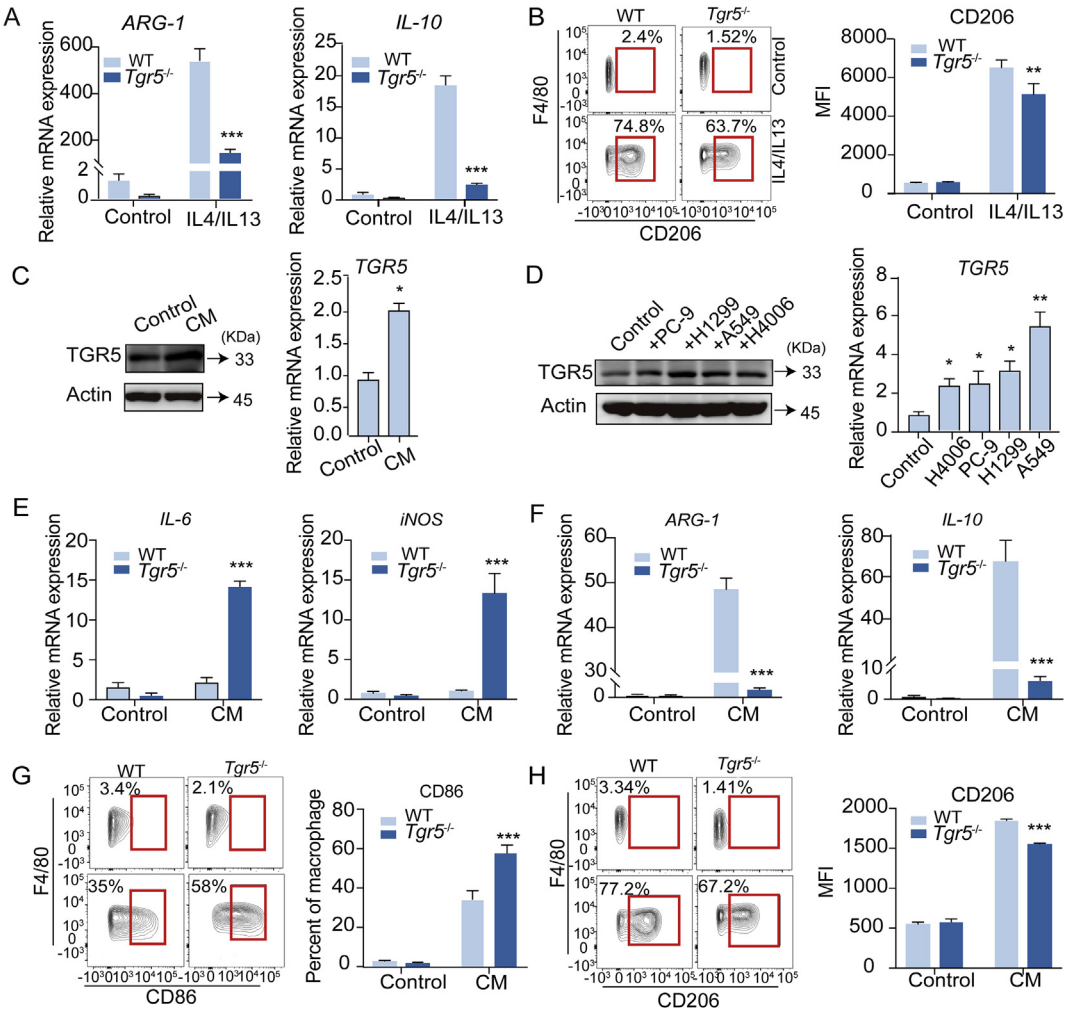

Figure 2 TGR5 deficiency in macrophages restrains the polarization to M2-like phenotypes. (A) Bone marrow derived macrophages (BMDMs) from WT and *Tgr5*$^{-/-}$ mice were treated with or without IL4/IL13 for 6 h. The expression of *ARG-1* and *IL-10* was measured by qPCR. (B) BMDMs were cultured in the presence of IL4/IL13 for 48 h. The percentage and mean fluorescence intensity of M2 macrophages (F4/80^{+}CD206^{+}) was determined by flow cytometry. (C) BMDMs were cultured with conditioned medium (CM) from LLC cells for 48 h (Western blot, left panel) and 6 h (qPCR, right panel), the expression of TGR5 was detection. (D) The expression of TGR5 in PMA-treated U937 macrophages incubated with CM from PC-9, H1299, A549 and HCC4006 cells for Western blot (48 h) and Q-PCR (6 h). WT and *Tgr5*$^{-/-}$ BMDMs were cocultured with LLC-CM for 6 h, mRNA expression of genes related to (E) inflammatory or (F) immunosuppressive macrophage polarization was detected by qPCR, with β-actin as control. (G) CD86 and (H) CD206 expression was measured by flow cytometry (48 h). Data are represented as mean ± standard deviation (SD) ($n = 3$). *P* values were determined by two-tailed Student's *t* test. *$P < 0.05$, **$P < 0.01$, ***$P < 0.001$, compared with the WT group.

enhanced macrophage phagocytosis and decreased macrophage-mediated tumor cell proliferation and migration.

3.4. *TGR5 deficiency restrains TAM-mediated CD8^{+} T cell suppression*

TAMs has the suppressive impact on T-cell proliferation and its associated antitumor activity. Thus, we co-cultured M2 macrophage or CM-treated macrophage with CD8^{+} T cells and evaluated the immunomodulatory effects of TGR5 in macrophages. We found that CD8^{+} T cells co-cultured with M2 macrophages derived from *Tgr5*$^{-/-}$ mice induced an increased ratio of activated CD8^{+} T cells over total CD8^{+} T cells. The increase in CD8^{+} T cells positive for either granzyme B, IFN-γ or TNF-α as compared with those in WT control further substantiated this notion (Fig. 4A–C). Similar results were obtained from CD8^{+} T cells co-cultured with tumor CM-treated macrophage derived from *Tgr5*$^{-/-}$ mice. There was an obvious upregulation of typical cytotoxic cytokines in CD8^{+} T cells following co-culture with CM-treated *Tgr5*$^{-/-}$ macrophage (Fig. 4D–F). However, under the same conditions, the CD8^{+} T-cell proliferation was similar between these two groups (Supporting Information Fig. S3). These data show that *Tgr5*$^{-/-}$ macrophages restrained TAM-mediated CD8^{+} T cell immune suppressive function, further revealing a crucial role of TGR5 on induction of immunosuppressive TAM rather than a direct impact on CD8^{+} T cell *per se*.

3.5. *Pharmacological inhibition of TGR5 decreases macrophage M2 polarization and activation*

To further confirm the role of TGR5 in macrophage M2-like polarization and its immunomodulatory impact, we applied a

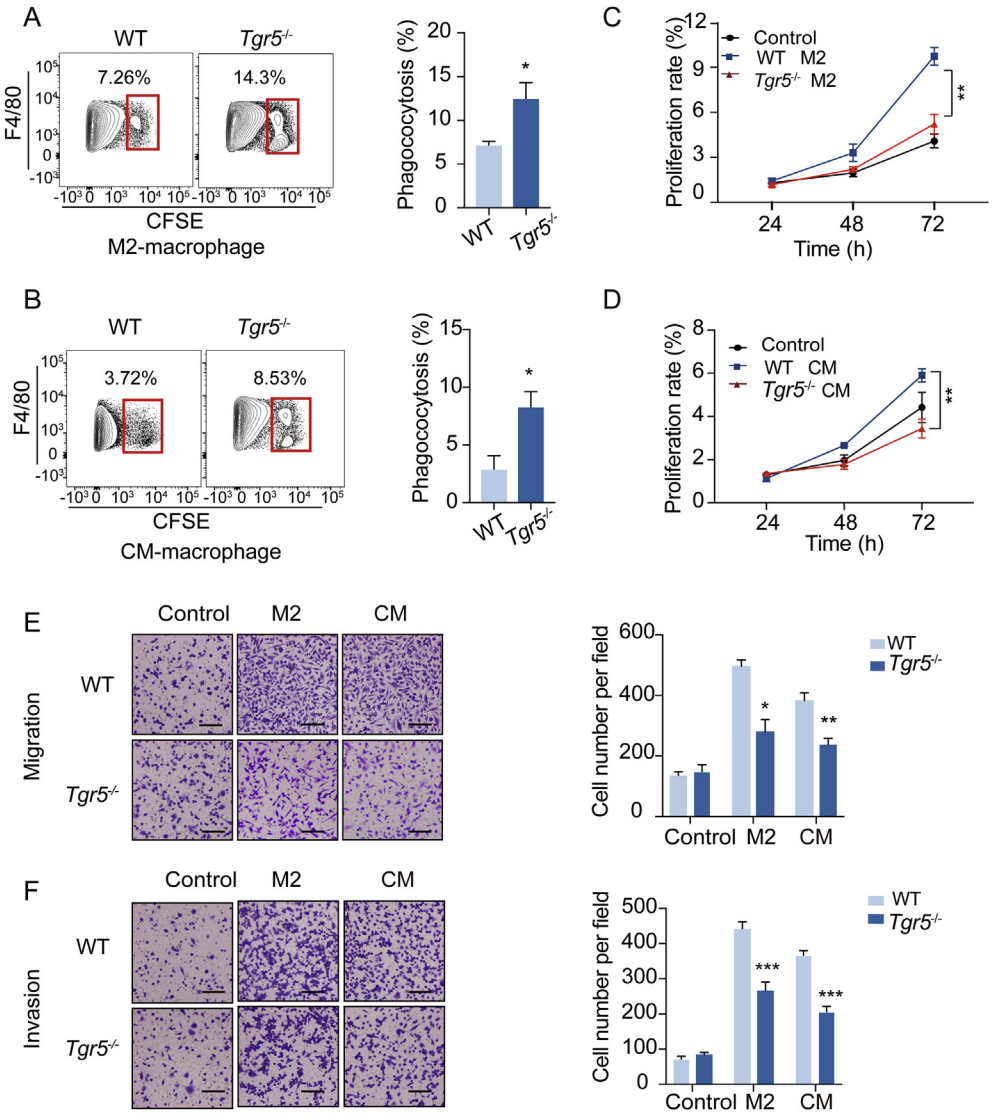

Figure 3 TGR5 deficiency enhances macrophage phagocytosis and decreases tumor-promoting properties. BMDMs (1×10^5) from WT and *Tgr5*$^{-/-}$ mice stimulated with IL-4/IL-13 or LLC CM for 48 h and then co-cultured with CFSE-labeled LLC (2×10^5) for 2 h. Phagocytosis of (A) M2 macrophages or (B) CM-macrophages assessed with flow cytometry. (C)−(F) The effect of TGR5 on macrophage-mediated tumor cell proliferation and migration. BMDMs from WT and *Tgr5*$^{-/-}$ mice were stimulated with IL-4/IL-13 or LLC-CM for 48 h, and the CM of macrophage was collected. LLC cells were cultured with (C) M2-CM or (D)TAM-CM. Cell proliferation was determined by using the SRB assay at different time points. LLC cells migrated (E) or invaded (F) into the lower chamber were evaluated by Transwell assay. Representative images were shown. Data are represented as mean ± SD ($n = 3$). *P* values were determined by two-tailed Student's *t* test. *$P < 0.05$, **$P < 0.01$, ***$P < 0.001$, compared with the WT group. Scale bar = 50 μm.

selective inhibitor for TGR5, known as SBI 115. BMDMs were pretreated with SBI 115 for 2 h and then stimulated with LLC-CM. We found that SBI 115 treatment significantly decreased the upregulation of M2 markers, accompanied by the increased expression of M1 marker (Fig. 5A). We further cultured PMA-U937 in CM collected from human cell lines, A549 and H1299. Similarly, we found that M1 surface markers, either *IL1-β* or *iNOS*, were upregulated, while M2 surface markers, including *ARG-1* and *IL-10*, were downregulated in SBI 115-treated groups (Fig. 5B and C). We also examined the effect of TGR5 inhibitor on the phagocytic capacity of macrophages. As expected, inhibition of TGR5 by SBI 115 resulted in increased tumor phagocytic capacity of CM-treated BMDMs (Fig. 5D) and M2-like macrophages (Supporting Information Fig. S4A). In addition, SBI 115 also strongly inhibited CM-macrophages induced LLC cell migration and invasion (Fig. 5E) in a dose-dependent manner. Similar results were also obtained in the M2 macrophages (Fig. S4B). We cultured $CD8^+$ T cells with LLC CM-educated BMDMs pretreated with or without SBI 115, and found that SBI 115 treatment dramatically increased the ratio of granzyme B expression in $CD8^+$ T cells (Fig. 5E). In addition, the expression of TNF-α or IFN-γ in $CD8^+$ T cells were obviously upregulated after co-culture with SBI 115-treated M2-macrophages (Fig. S4C). Thus, pharmacological inhibition of TGR5 effectively attenuated M2 macrophages polarization in the TME and promoted an antitumor immune response.

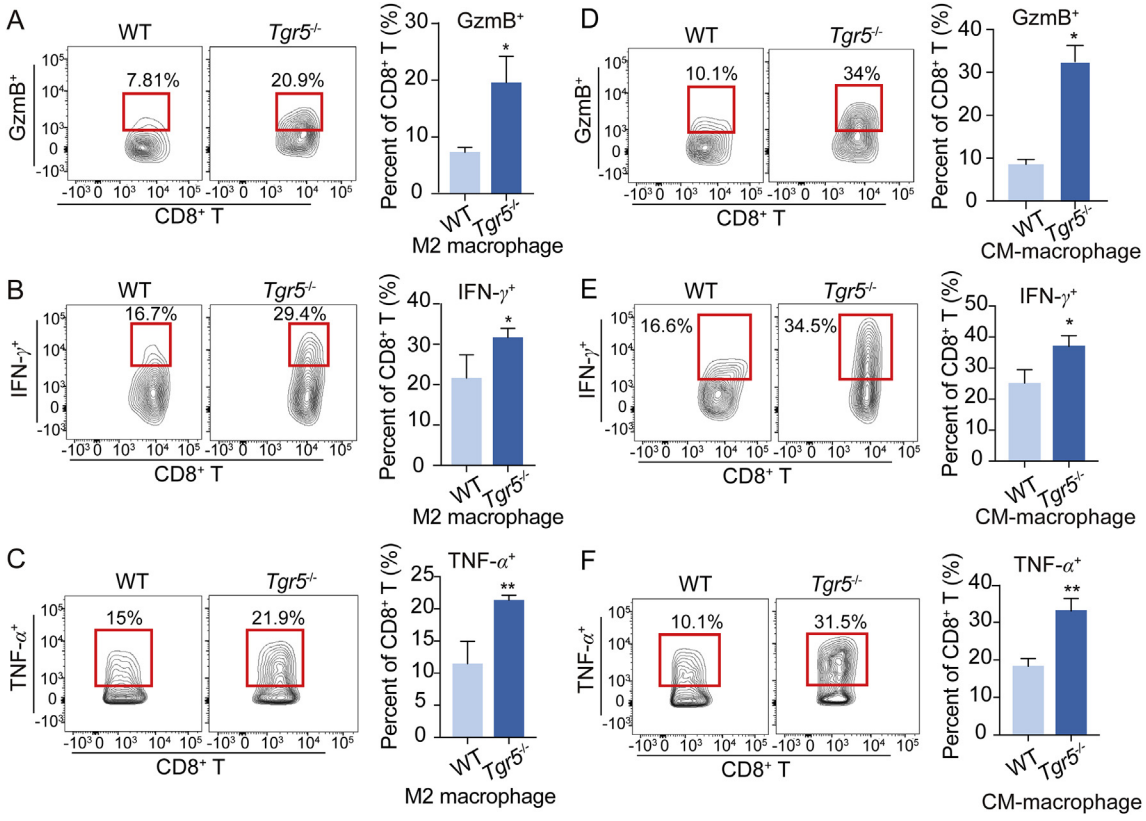

Figure 4 TGR5 deficiency restrains TAM-mediated $CD8^+$ T cell suppression. TGR5 deficiency in macrophages restored co-cultured $CD8^+$ T cell functions. Macrophages (1×10^5) derived from WT and $Tgr5^{-/-}$ mice were stimulated with (A)−(C) IL-4/IL-13 or (D)−(F) LLC-CM for 48 h, and then cocultured with $CD8^+$ T cell ($5-10 \times 10^5$) for 72 h. Typical cytotoxic cytokines in $CD8^+$ T cells: granzyme B (GzmB), IFN-γ and TNF-α were assessed with flow cytometry. Data are represented as mean ± SD ($n = 3$). P values were determined by two-tailed Student's t test. $^*P < 0.05$, $^{**}P < 0.01$, compared with the WT group.

3.6. TGR5 induces macrophage M2 polarization via activating cAMP-STAT3/STAT6 signaling

Next, we asked how TGR5 reprogramed "protumor" TAMs phenotypes. TGR5 is a G-protein-coupled bile acid receptor that transmits bile acid signaling *via* the intracellular cAMP signaling pathway, leading to reduced lipopolysaccharide-mediated cytokine production[27]. Meanwhile, the activation of cAMP was reported to increase M2 macrophage[28]. We hence measured the production of cAMP and found that WT-BMDMs treated with IL4/IL13 or LLC-CM showed an increase in cAMP level, which was decreased in $Tgr5^{-/-}$ BMDMs cells (Fig. 6A). Likewise, SBI 115 treatment also inhibited cAMP production in BMDMs (Fig. 6B). We also examined the most known signaling molecules involved in macrophage activation, including CREB, STAT6, STAT3, SOCS, AKT and ERK. Despite a marginal influence in SOCS, p-AKT and p-ERK, the phosphorylation of CREB, STAT6 and STAT3 were all remarkably decreased in $Tgr5^{-/-}$ macrophage stimulated with IL4/IL13 or LLC-CM (Fig. 6C). This finding was recapitulated using SBI 115 treatment (Fig. 6D). These results show the decreased cAMP−STAT3/STAT6 signaling axis in TGR5 deficient macrophages. To test whether the decreased cAMP accounts for the STAT3/STAT6 signaling and the associated M2-like phenotype of macrophage, we pretreated macrophages with forskolin, an adenylyl cyclase activator that can effective increased cAMP production both in $Tgr5^{-/-}$ and WT macrophages (Supporting Information Fig. S5A−S5D). Next, we found the elevation of intracellular cAMP partially rescued the decrease in p-STAT3 and p-STAT6 levels caused by TGR5 deficiency in macrophages (Fig. 6E, Fig. S5E and S5F). Importantly, forskolin also restored the levels of *ARG-1* and *IL-10* in $Tgr5^{-/-}$ macrophages (Fig. 6F−H), and the suppressed LLC cell proliferation and migration ability caused by TGR5 deficiency BMDMs were also restored by the pretreatment with forskolin (Fig. S5G−S5H). These results together suggest that TGR5 induced macrophage M2 polarization *via* activating cAMP−STAT3/STAT6.

As a membrane receptor for bile acids, TGR5 can be activated by a wide range of ligands, including all known bile acids. To clarify whether peripheral bile acid affects the regulatory effect of TGR5 on macrophage polarization, BMDMs from $Tgr5^{-/-}$ mice or WT mice were stimulated with different dosage of chenodeoxycholic acid (CDCA), and we found that the mRNA expression levels of M1 macrophage signature genes, including *IL-6* and *iNOS*, were obviously down-regulated in a dose-dependent manner (Supporting Information Fig. S6A and S6B). In contrast, the expression of M2 macrophage-associated genes (*IL-10* and *ARG-1*) were significantly upregulated upon CDCA stimulation (Fig. S6C and S6D). Importantly, the impact of CDCA was abolished in $Tgr5^{-/-}$ BMDMs. Likewise, CDCA treatment increased the induction of anti-inflammatory genes in WT BMDM by LLC-CM but failed to do the same in $Tgr5^{-/-}$ BMDM (Fig.

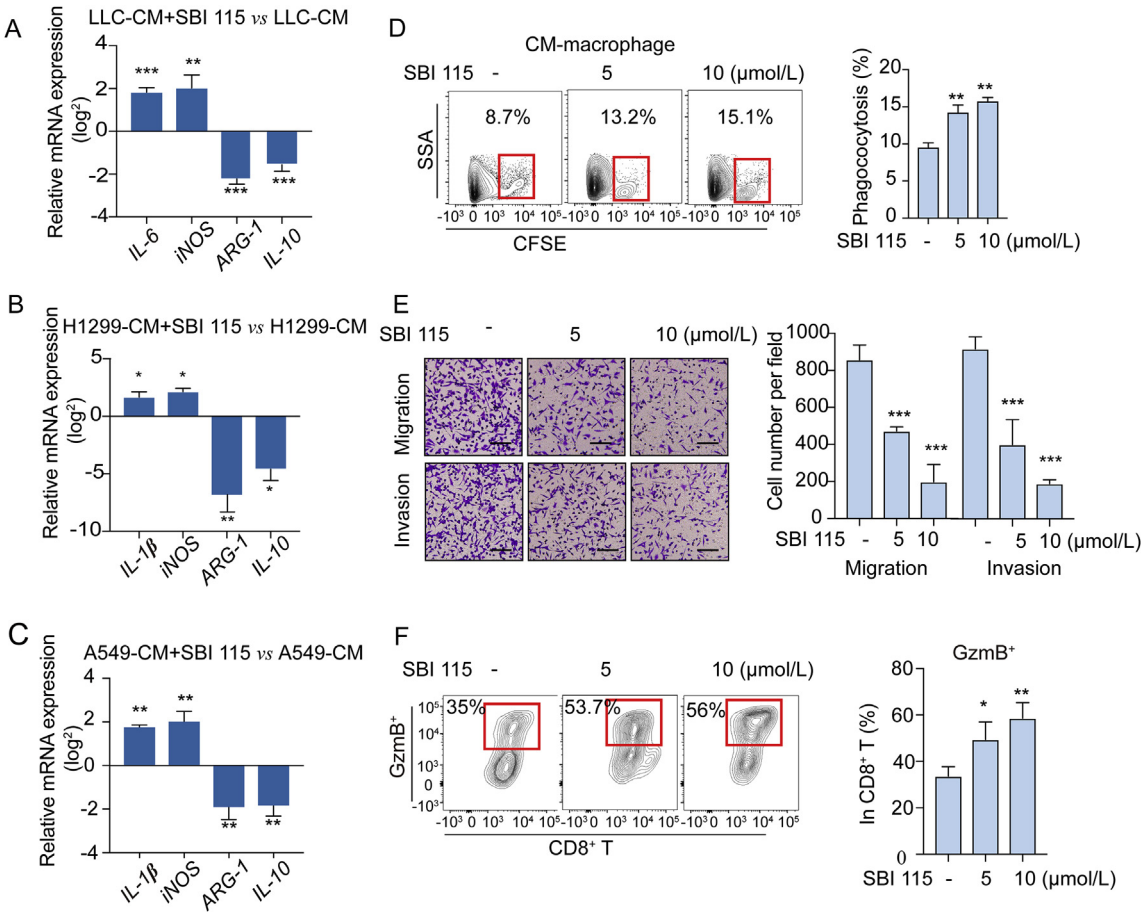

Figure 5 Pharmacological inhibition of TGR5 decreases macrophage M2 polarization and activation. (A)−(C) TGR5 inhibition suppresses M2 macrophage subtype differentiation. BMDMs and PMA-treated U937 were cultured with CM from tumor cells with or without SBI 115. mRNA expression of genes related to M1 or M2 macrophage activation was detected by qPCR. Data were normalized to those without SBI 115 treatment, and represented in $\log^2$ scale, with β-actin as control. (D)−(F) TGR5 inhibition promoted an antitumor immune response. BMDMs were treated with LLC-CM with or without SBI 115 for 48 h and then cocultured with LLC. (D) Phagocytosis of CM-macrophages assessed with flow cytometry. (E) Transwell migration assays of LLC cells. (F) LLC-CM-macrophage pretreated with SBI 115 and then cocultured with $CD8^+$ T cell. Granzyme B (GzmB) was assessed with flow cytometry. Data are represented as mean ± SD ($n = 3$). *P* values were determined by two-tailed Student's *t* test. $^*P < 0.05$, $^{**}P < 0.01$, $^{***}P < 0.001$, compared with the control. Scale bar = 50 μm.

S6E and S6F), indicating that CDCA induced macrophage phenotype shift and promoted M2 polarization in a TGR5-dependent manner in NSCLC.

3.7. *$Tgr5^{-/-}$ BMDM inhibits LLC tumor growth and enhances antitumor immunity*

Given the role of TGR5 in reprograming TAMs and restraining TAM-mediated tumor-promoting effects, we sought to investigate whether *$Tgr5^{-/-}$* BMDMs would reshape TME and exhibit antitumor effect *in vivo*. To this end, *$Tgr5^{-/-}$* or WT BMDMs were mixed with LLC cells and then inoculated into C57BL/6J mice with pre-depletion of macrophages. LLC xenograft containing *$Tgr5^{-/-}$* macrophage displayed a slow tumor growth compared with the those mixed with WT macrophage (Fig. 7A and B). Next, we investigated whether *$Tgr5^{-/-}$* macrophage also influenced TAMs turnover and infiltration of other immune cell subpopulations, especially $CD8^+$ T cells in TME. Analysis of tumor infiltrating immune cells showed that the frequency of total hematopoietic cells ($CD45^+$) did not differ between the two groups. TAMs had a decrease tendency in *$Tgr5^{-/-}$* macrophage cocultured LLC group, but it did not reach statistical significance (Fig. 7C and D). In contrast, the proportion of $CD86^+$ M1 macrophages was increased with the markedly decrease of $CD206^+$ M2 macrophages infiltration (Fig. 7E and F). These results suggest that TGR5 remodeled TAM from tumor-promoting M2-like phenotypes into "antitumor" M1-like phenotypes. Along with the phenotypic transformation of TAMs, tumors bearing *$Tgr5^{-/-}$* macrophage exhibited obviously elevated MHC II expression on DC (Fig. 7G) and proportions of IFN-γ^+ $CD4^+$ T cells (Fig. 7H), indicating the increase DC activation and Th1-dominant responses. Meanwhile, IFN-γ^+CD8^+ T cells (Fig. 7I) and granzyme B^+CD8^+ T cells (Fig. 7J) were also expanded in *$Tgr5^{-/-}$* macrophage group, with reduced PD-1^+CD8^+ T cells population (Fig. 7K), although it did not affect the $CD8^+$ T cells infiltration (Supporting Information Fig. S7A). In addition, IHC analysis also confirmed less CD206 in *$Tgr5^{-/-}$* group (Fig. S7B). All these findings demonstrated that *$Tgr5^{-/-}$* BMDM remodeled the immunosuppressive TME to enhance antitumor immunity in TME.

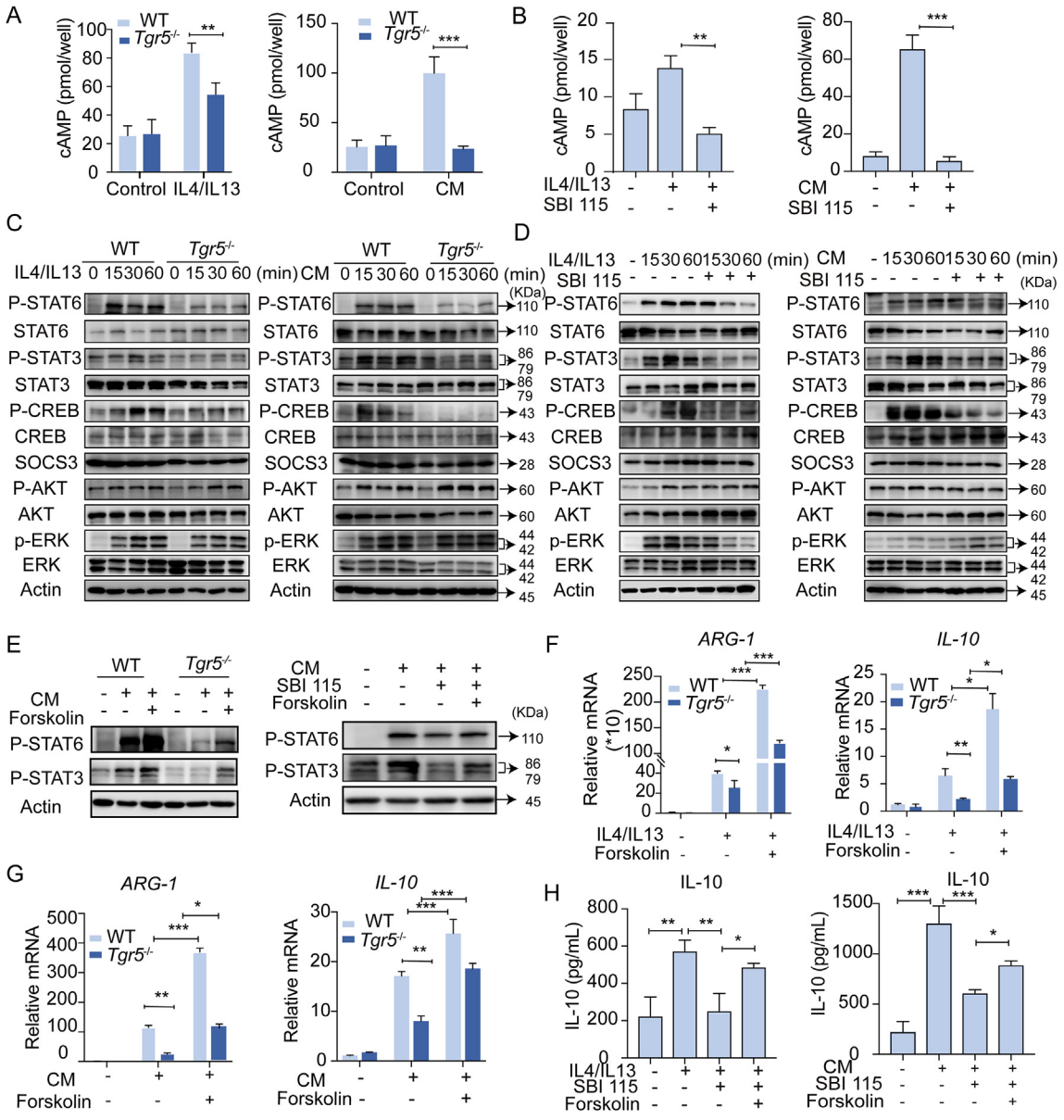

Figure 6 TGR5 induces macrophage M2 polarization *via* activating cAMP−STAT3/STAT6 signaling. (A) WT and *Tgr5*$^{-/-}$ BMDMs were stimulated with IL4/IL13 (left panel) or LLC-CM (right panel) for 2 h, and cAMP production was assessed. (B) BMDMs from C57BL/6J mice were pretreated with SBI-115 (10 μmol/L) in the presence of IL4/IL13 (left panel) or LLC-CM (right panel) for 2 h, cells were lysed and cAMP measured according to the manufacturers kit instructions. (C) WT and *Tgr5*$^{-/-}$ BMDMs were stimulated with IL4/IL13 (left panel) or LLC-CM (right panel) for the indicated times, and then cell lysates were subjected to SDS-PAGE and immunoblotted to detect the indicated proteins. (D) BMDMs were pretreated with SBI-115 (10 μmol/L) in the presence of IL4/IL13 (left panel) or LLC-CM (right panel) for the indicated times. (E) *Tgr5*$^{-/-}$ or WT BMDMs were treated with forskolin (50 μmol/L) in the presence of LLC-CM for 30 min, and cells were lysed and subjected to SDS-PAGE for immunoblotting for p-STAT3 and p-STAT6. (F) and (G) WT and *Tgr5*$^{-/-}$ macrophages were pretreated with forskolin, followed by treatment with IL4/IL13 for 6 h, *ARG-1* and *IL-10* expression was measured. (H) BMDMs were pretreated with SBI-115 (10 μmol/L) and forskolin in the presence of IL4/IL13 or LLC-CM for 48 h, and the expression of IL10 were measured by ELISA. Data are represented as mean ± SD ($n = 3$). *P* values were determined by one-way analysis of variance (ANOVA). *$P < 0.05$; **$P < 0.01$; ***$P < 0.001$.

3.8. Concurrent TGR5 expression and TAMs infiltration predicts poor prognosis and shorter OS in NSCLC

Considering the important regulatory role of TGR5 in TAMs and immune suppression in murine models, we further explored its prognostic value in NSCLC patients. First, we examined the correlation between TGR5 expression and TAMs signature in NSCLC clinical specimens. Our data show that the expression of CD68, the biomarker of TAMs, was obviously higher in the TGR5-high tumor sites than in the TGR5-low tumor sites (Fig. 8A and B). Correlation analysis revealed a statistically significant positive correlation between TGR5 and TAMs infiltration in NSCLC samples (Table 1). These results were further confirmed by extended analyses of the TCGA database, similarly supporting

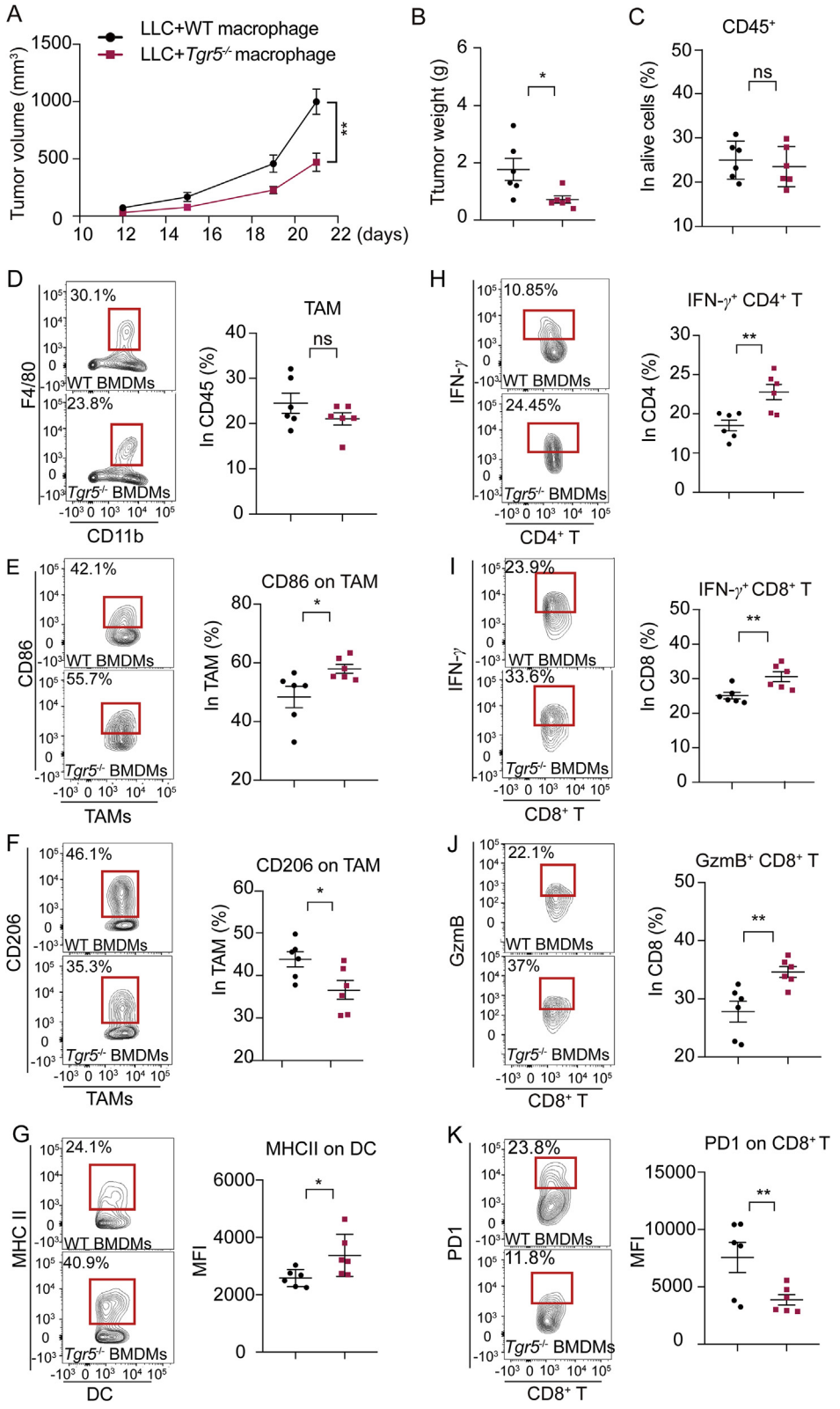

Figure 7 $Tgr5^{-/-}$ BMDM inhibits LLC tumor growth and enhances antitumor immunity. LLC cells (2×10^6) mixed with WT or $Tgr5^{-/-}$ macrophages (5×10^5) were injected subcutaneously into C57BL/6J mice with pre-depletion of macrophages. (A) The tumor volume and (B) tumor weight are shown on the indicated days. (C)−(K) Flow cytometric analysis of immune subsets in the tumor microenvironment. (C) The infiltration of $CD45^+$ cell among live cell. The infiltration of (D) TAMs ($CD11b^+$ $F4/80^+$), (E) $CD86^+$ TAMs, (F) $CD206^+$ TAMs, (G) the expression of MHC on DC, (H) IFN-γ^+ $CD4^+$ T cells, (I) IFN-γ^+ $CD8^+$ T cells, (J) $GzmB^+$ $CD8^+$ Tells and (K) $PD1^+$ $CD8^+$ T cells were tested. Data are represented as mean ± standard error of mean (SEM) ($n = 6$). P values were determined by two-tailed Student's t test. *$P < 0.05$, **$P < 0.01$; ns, not significant, compared with the WT-BMDMs group.

that TGR5 high-expression was associated with high TAM ($CD68^+$) infiltration, especially M2-like TAM ($CD206^+$) infiltration in both LUSC and LUAD (Fig. 8C and D). Next, we investigated the prognostic impact of TGR5 and TAMs infiltration and revealed that patients concurrent with TGR5-high and high TAMs infiltration predicated a poor prognosis, with shorter 5-year-survival rate, as compared with patients with "TGR5-high, low-infiltration-TAMs" or "TGR5-low, low-infiltration-TAMs" tumor in NSCLC (Fig. 8E). Meanwhile, we found TGR5 was also positive in stromal cells that are mainly consisted of macrophages and if these samples were re-graded by TGR5 positive in stromal cells, we found that elevated amounts of $CD68^{positive}TGR5^{positive}$ stromal cells infiltration implicated significantly shorter survival time of patients than those expressing $CD68^{positive}TGR5^{negative}$ stromal cells (Supporting Information Fig. S8A and S8B). Above data indicate that TGR5-high tumors with high TAMs were associated with poor prognosis in lung cancer.

4. Discussion

TAMs are a major component of the TME and show considerable functional and phenotypic plasticity in response to different stimuli. In most cancers, their presence tends to be a negative prognostic indicator, as TAMs in established tumors are generally skewed toward the protumorigenic M2 phenotype, promoting tumor progression and suppressing anti-tumor immune response[14,29]. Therefore, TAMs have been considered an important target for anti-tumor immunotherapy. In this work, we reveal an important regulatory role of TGR5 in TAMs in NSCLC, in which TGR5 plays a key role in eliciting macrophage immunosuppressive phenotype and inhibiting antitumor immune response in TME. Therefore, we identify TGR5 as a promising target in TAMs targeting antitumor immunotherapy in NSCLC.

TGR5 is a bile acid receptor and exerts a potent anti-inflammatory effect of macrophage in various inflammatory-related diseases. Our data indicate that TGR5 was not only required in typical M2 polarization of macrophages but also facilitated cancer cell-induced immunosuppressive phenotype of macrophage in TME (Fig. 2 and Fig. S2). Additionally, TGR5 knockdown or inhibition in macrophage led to more abundant pro-inflammatory subtype of macrophages (Figs. 2 and 5). Previous studies have shown the potential pharmacological intervention of TGR5 for the treatment of inflammatory disorders[18,30–32]. In this study, we focused on exploring the participation of TGR5 in reprograming TAMs and thereby promoting immune suppression in NSCLC. In addition to the suppressed tumor growth, our study found $Tgr5^{-/-}$ mice exhibited a decrease in TAM and $CD206^+$ TAM but an increase in IFN-γ^+ $CD8^+$ T as compared to LLC-WT mice, suggesting that TGR5 exerted an immunosuppressive effect in the tumor microenvironment (Fig. 1). Moreover, our *in vitro* results demonstrated that TGR5 was not only promoted TAMs polarization into a protumoral state but also altered macrophages tumor phagocytosis and blocked macrophage-mediated cancer cell migration and invasion (Fig. 3, and Fig. S2). In addition, $Tgr5^{-/-}$ macrophage suppressed tumor progression and enhanced anti-tumor immunity *in vivo*, characterized by a dramatic reduction in tumor-infiltrating M2-like TAMs, increased infiltration of anti-tumor lymphoid cell populations, such as mature DC cells and $CD4^+$ effector T cells, as well as activated $CD8^+$ T cells (Fig. 7). This result was in line with previous studies showing that reprogramming TAMs could overcome TAMs-induced immunosuppression and tumor growth[33,34]. As mentioned above, the tumor immune microenvironment determined the response to various immunotherapeutic approaches[35]. Reprogramming cells in the immune compartment, such as immunosuppressive TAMs, may overcome microenvironment-induced drug resistance and enhance antitumor immunity[25,36,37]. TGR5 may be a viable target for enhancing immunotherapies. However, further investigation of combination strategy is needed to confirm this hypothesis.

Our previous studies have found that TGR5 in cancer cell involved in cell proliferation both *in vitro* and *in vivo* and TGR5 knockdown induced cell cycle arrest at G1/S phase and blocked cell cycle progression in NSCLC[24]. Another study also showed that bile acids increase cell proliferation of gastric cancer cells *via* activation of TGR5 receptors and $G_q\alpha$ and $G\alpha i$-3 proteins[22]. Moreover, Li et al.[38] indicated that mortalin may be a downstream component regulated by TGR5, and TGR5 promoted cholangiocarcinoma cell proliferation partially by interacting with mortalin. In contrast to patients with gastric, cholangiocarcinoma and lung cancer, the binding of bile acids to TGR5 induced c-Jun-N terminal kinase (JNK) activation and enhanced apoptosis in hepatocytes[39]. However, TGR5 seems to have a less effect on the proliferation and survival of TAMs (Fig. S1). Similar to our results, Perino et al.[30] also found that blood differentiation counts of $Tgr5^{-/-}$ mice did not have any significant effect caused by loss of TGR5 in monocytes or other leukocytes. These findings indicate that the different roles of TGR5 in regulating cell proliferation might highly cell type-dependent and context-dependent manner in cancer.

How TGR5 is activated *in vivo* in cancer patients also aroused our interest. We have previously showed that serum levels of DCA, CDCA and UDCA in NSCLC patients were higher than those of the healthy subjects[24], suggesting that blood bile acid could activate TGR5. We further find CDCA induced-macrophage phenotype shift was TGR5-dependent and CDCA treatment increased LLC-CM-induced the expression of anti-inflammatory genes (Fig. S6). Thus, we speculate that the increased blood bile acid in NSCLC patients, especially CDCA, attenuated M1 polarization and increased M2 polarization in a TGR5-dependent manner in NSCLC. Another unanswered question is why TGR5 expression was induced by CM from tumor cell culture. Xiong et al.[40] demonstrated that viral infection or IFN-β treatment upregulates TGR5 expression in an IFN/STAT1-dependent manner, which can be recognized as an interferon-stimulated gene (ISG). Several studies also showed the transcription of TGR5 was increased in microglia treated with LPS[41]. Based on these insights, we speculate that lung cancer cells can produce a large amount of secreted proteins such as IFN-β into the CM to induce the expression of TGR5. This hypothesis needs validation in further work.

The second messenger cAMP is stimulated by a variety of extracellular stimuli through GPCRs[42]. TGR5 has been reported to trigger the cAMP-dependent pathway involved in bile acid-induced NLRP3 inflammasome inhibition[43], reducing macrophage inflammation and lipid loading[16] and regulating nuclear factor-κB P65 activation in Crohn's disease[19]. Moreover, cAMP has a synergistic effect with IL-4 on STAT6 expression and may serve as a co-factor in macrophage reprogramming. In the present study, we further confirmed that cAMP was involved in TGR5-mediated TAMs differentiation in the TME. Most known signaling molecules involved in M2 macrophage function, such as

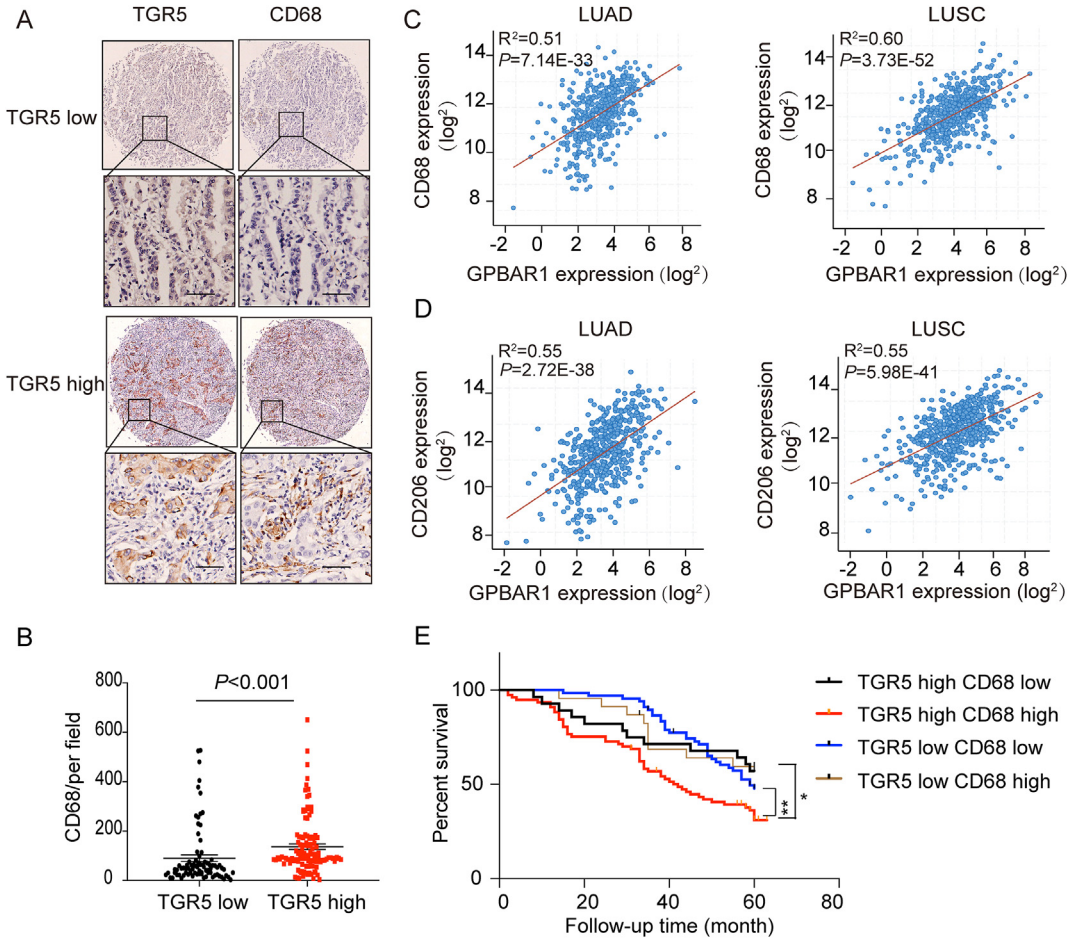

Figure 8 Concurrent TGR5 expression and infiltration of TAMs predict poor prognosis and shorter OS in NSCLC. IHC staining was performed to determine the correlation between TGR5 expression and TAMs infiltration in 200 NSCLC lung tissues. (A) Representative immunostaining images of TGR5 and TAM ($CD68^+$) infiltration in NSCLC samples are shown at low (30×) and high (200×) magnifications (scale bar, 50 μm). (B) TGR5-high tumors ($n = 109$) are associated with increased TAM ($CD68^+$) infiltration compared with TGR5-low tumors ($n = 91$, $P < 0.001$, Mann−Whitney U test). Correlation between TGR5 (GPBAR1) expression and CD68 (C) and CD206 (D) in 1032 patients from the TCGA database. LUSC, lung squamous cell carcinoma; LUAD, lung adenocarcinoma; *P* values and *R* values were calculated based on Pearson's correlation analysis. (E) Kaplan−Meier survival curves of TGR5-low/CD68-low ($n = 67$), TGR5-low/CD68-high ($n = 24$), TGR5-high/CD68-low ($n = 31$), and TGR5-high/CD68-high ($n = 78$) NSCLC patients (TGR5-high/CD68-high *vs.* TGR5-low/CD68-low, $P = 0.0037$; TGR5-high/CD68-high *vs.* TGR5-high/CD68-low, $P = 0.02$, log-rank test). *$P < 0.05$, **$P < 0.01$.

Table 1 Correlation analysis between TGR5 and CD68 expression in NSCLC.

NSCLC samples	CD68		Correlation coefficient	*P* value
	Low	High		
TGR5 low	67	24	0.45	<0.001[a]
TGR5 high	31	78		

[a]Data were analyzed using the χ^2 test.

the phosphorylation of CREB, STAT3 and STAT6 were remarkably decreased in *Tgr5*$^{-/-}$ macrophage stimulated with IL4/IL13 or LLC-CM. Moreover, induction of cAMP production restored M2-like phenotypes in *Tgr5*-deficient macrophage. Our results indicate that TGR5 deficiency in TAMs restrains macrophage polarization towards M2-like protumor phenotypes *via* diminishing cAMP−STAT3/STAT6 signaling (Fig. 6). Abundant literature has revealed that STAT3 and STAT6 are highly activated in tumor macrophages and have been shown to promote lung cancer progression[44–46]. Accordingly, increasing STAT3 and STAT6 expression in TAMs resulted in impaired cytotoxic T lymphocyte activation, decreasing immunotherapy efficacy[47]. STAT3 and STAT6 may be involved in the mechanism by which TGR5 reshapes the TME.

To date, numerous studies have showed that the localization and density of TAMs are associated with poor clinical outcome in lung cancer and are independent prognostic markers in NSCLC patients[48]. Our study discovered high TGR5 expression associated with high TAMs infiltration predicts the poor prognosis in NSCLC. TGR5 high-expression was associated with high TAM ($CD68^+$), especially M2-like TAM in NSCLC. Moreover, the TGR5-high tumors concurred with a high TAM had a poor prognosis, with shorter 5-year-OS rate in NSCLC (Fig. 8).

Together, this study provides molecular mechanisms for the protumor function of TGR5 in NSCLC, highlighting its potential as a target for TAM-centric immunotherapy in NSCLC.

5. Conclusions

Our results indicate the important regulatory role of TGR5 in TAMs. It facilitates macrophage immunosuppressive phenotype, inhibits antitumor immune response and promotes tumor progression in NSCLC. Therefore, TGR5 is a promising drug target for TAM-centric anti-tumor immunotherapy in NSCLC, which might potentially benefit the population refractory to immune checkpoint blockade (ICB) therapeutics.

Acknowledgments

We thank Dr. Jing Ai (Shanghai Institute of Materia Medica, Chinese Academy of Sciences, Shanghai, China) and other members of Dr. Jing Ai's laboratory for their assistance in the project. This work was supported by the National Natural Science Foundation of China (81874314 and 81903633) and "Yangfan" project of Shanghai Science and Technology Commission (19YF1428700, China).

Author contributions

Handong Jiang and Jing Zou designed the research. Lifang Zhao and Hongyan Zhang carried out the experiments, Xueqing Liu performed data analysis. Shan Xue and Dongfang Chen assisted with carrying out experiments. Lifang Zhao and Xueqing Liu wrote the manuscript. Handong Jiang revised the manuscript. All of the authors have read and approved the final manuscript.

Conflicts of interest

Authors declare no conflict of interest.

Appendix A. Supporting information

Supporting data to this article can be found online at https://doi.org/10.1016/j.apsb.2021.07.011.

References

1. Siegel RL, Miller KD, Jemal A. Cancer statistics. 2019 *CA Cancer J Clin* 2019;**69**:7−34.
2. Arbour KC, Riely GJ. Systemic therapy for locally advanced and metastatic non-small cell lung cancer: a review. *J Am Med Assoc* 2019;**322**:764−74.
3. Boumahdi S, de Sauvage FJ. The great escape: tumour cell plasticity in resistance to targeted therapy. *Nat Rev Drug Discov* 2020;**19**:39−56.
4. Chae YK, Arya A, Iams W, Cruz MR, Chandra S, Choi J, et al. Current landscape and future of dual anti-CTLA4 and PD-1/PD-L1 blockade immunotherapy in cancer; lessons learned from clinical trials with melanoma and non-small cell lung cancer (NSCLC). *J Immunother Cancer* 2018;**6**:39.
5. Locati M, Curtale G, Mantovani A. Diversity, mechanisms, and significance of macrophage plasticity. *Annu Rev Pathol* 2020;**15**:123−47.
6. Ngambenjawong C, Gustafson HH, Pun SH. Progress in tumor-associated macrophage (TAM)-targeted therapeutics. *Adv Drug Deliv Rev* 2017;**114**:206−21.
7. Franklin RA, Liao W, Sarkar A, Kim MV, Bivona MR, Liu K, et al. The cellular and molecular origin of tumor-associated macrophages. *Science* 2014;**344**:921−5.
8. Shu Y, Cheng P. Targeting tumor-associated macrophages for cancer immunotherapy. *Biochim Biophys Acta Rev Cancer* 2020;**1874**:188434.
9. Cassetta L, Pollard JW. Targeting macrophages: therapeutic approaches in cancer. *Nat Rev Drug Discov* 2018;**17**:887−904.
10. Mantovani A, Marchesi F, Malesci A, Laghi L, Allavena P. Tumour-associated macrophages as treatment targets in oncology. *Nat Rev Clin Oncol* 2017;**14**:399−416.
11. Wang Y, Lin YX, Qiao SL, An HW, Ma Y, Qiao ZY, et al. Polymeric nanoparticles promote macrophage reversal from M2 to M1 phenotypes in the tumor microenvironment. *Biomaterials* 2017;**112**:153−63.
12. Mantovani A, Allavena P. The interaction of anticancer therapies with tumor-associated macrophages. *J Exp Med* 2015;**212**:435−45.
13. Ries CH, Cannarile MA, Hoves S, Benz J, Wartha K, Runza V, et al. Targeting tumor-associated macrophages with anti-CSF-1R antibody reveals a strategy for cancer therapy. *Cancer Cell* 2014;**25**:846−59.
14. Conway EM, Pikor LA, Kung SH, Hamilton MJ, Lam S, Lam WL, et al. Macrophages, inflammation, and lung cancer. *Am J Respir Crit Care Med* 2016;**193**:116−30.
15. Kawamata Y, Fujii R, Hosoya M, Harada M, Yoshida H, Miwa M, et al. A G protein-coupled receptor responsive to bile acids. *J Biol Chem* 2003;**278**:9435−40.
16. Pols TW, Nomura M, Harach T, Lo Sasso G, Oosterveer MH, Thomas C, et al. TGR5 activation inhibits atherosclerosis by reducing macrophage inflammation and lipid loading. *Cell Metabol* 2011;**14**:747−57.
17. Lewis ND, Patnaude LA, Pelletier J, Souza DJ, Lukas SM, King FJ, et al. A GPBAR1 (TGR5) small molecule agonist shows specific inhibitory effects on myeloid cell activation *in vitro* and reduces experimental autoimmune encephalitis (EAE) *in vivo*. *PLoS One* 2014;**9**:e100883.
18. Biagioli M, Carino A, Cipriani S, Francisci D, Marchianò S, Scarpelli P, et al. The bile acid receptor GPBAR1 regulates the M1/M2 phenotype of intestinal macrophages and activation of GPBAR1 rescues mice from murine colitis. *J Immunol* 2017;**199**:718−33.
19. Yoneno K, Hisamatsu T, Shimamura K, Kamada N, Ichikawa R, Kitazume MT, et al. TGR5 signalling inhibits the production of pro-inflammatory cytokines by *in vitro* differentiated inflammatory and intestinal macrophages in Crohn's disease. *Immunology* 2013;**139**:19−29.
20. Yang J, Hu J, Feng L, Yi S, Ye Z, Lin M, et al. Decreased expression of TGR5 in Vogt-Koyanagi-Harada (VKH) disease. *Ocul Immunol Inflamm* 2020;**28**:200−8.
21. Hong J, Behar J, Wands J, Resnick M, Wang LJ, DeLellis RA, et al. Role of a novel bile acid receptor TGR5 in the development of oesophageal adenocarcinoma. *Gut* 2010;**59**:170−80.
22. Cao W, Tian W, Hong J, Li D, Tavares R, Noble L, et al. Expression of bile acid receptor TGR5 in gastric adenocarcinoma. *Am J Physiol Gastrointest Liver Physiol* 2013;**304**:G322−7.
23. Chen MC, Chen YL, Wang TW, Hsu HP, Lai MD. Membrane bile acid receptor TGR5 predicts good prognosis in ampullary adenocarcinoma patients with hyperbilirubinemia. *Oncol Rep* 2016;**36**:1997−2008.
24. Liu X, Chen B, You W, Xue S, Qin H, Jiang H. The membrane bile acid receptor TGR5 drives cell growth and migration *via* activation of the JAK2/STAT3 signaling pathway in non-small cell lung cancer. *Cancer Lett* 2018;**412**:194−207.
25. You W, Li L, Sun D, Liu X, Xia Z, Xue S, et al. Farnesoid X receptor constructs an immunosuppressive microenvironment and sensitizes $FXR^{high}PD\text{-}L1^{low}$ NSCLC to anti-PD-1 immunotherapy. *Cancer Immunol Res* 2019;**7**:990−1000.
26. Zhao L, Xia J, Li T, Zhou H, Ouyang W, Hong Z, et al. Shp 2 deficiency impairs the inflammatory response against haemophilus influenzae by regulating macrophage polarization. *J Infect Dis* 2016;**214**:625−33.
27. Ichikawa R, Takayama T, Yoneno K, Kamada N, Kitazume MT, Higuchi H, et al. Bile acids induce monocyte differentiation toward interleukin-12 hypo-producing dendritic cells *via* a TGR5-dependent pathway. *Immunology* 2012;**136**:153−62.
28. Polumuri S, Perkins DJ, Vogel SN. cAMP levels regulate macrophage alternative activation marker expression. *Innate Immun* 2020;**27**:133−42.

29. Qian BZ, Pollard JW. Macrophage diversity enhances tumor progression and metastasis. *Cell* 2010;**141**:39−51.
30. Perino A, Pols TW, Nomura M, Stein S, Pellicciari R, Schoonjans K. TGR5 reduces macrophage migration through mTOR-induced C/EBPβ differential translation. *J Clin Invest* 2014;**124**:5424−36.
31. Zhou H, Zhou S, Shi Y, Wang Q, Wei S, Wang P, et al. TGR5/Cathepsin E signaling regulates macrophage innate immune activation in liver ischemia and reperfusion injury. *Am J Transplant* 2021;**21**:1453−64.
32. Rao J, Yang C, Yang S, Lu H, Hu Y, Lu L, et al. Deficiency of TGR5 exacerbates immune-mediated cholestatic hepatic injury by stabilizing the β-catenin destruction complex. *Int Immunol* 2020;**32**:321−34.
33. Tan B, Shi X, Zhang J, Qin J, Zhang N, Ren H, et al. Inhibition of Rspo-Lgr4 facilitates checkpoint blockade therapy by switching macrophage polarization. *Cancer Res* 2018;**78**:4929−42.
34. Wang R, Liu Y, Liu L, Chen M, Wang X, Yang J, et al. Tumor cells induce LAMP2a expression in tumor-associated macrophage for cancer progression. *EBioMedicine* 2019;**40**:118−34.
35. Datta M, Coussens LM, Nishikawa H, Hodi FS, Jain RK. Reprogramming the tumor microenvironment to improve immunotherapy: emerging strategies and combination therapies. *Am Soc Clin Oncol Educ Book* 2019;**39**:165−74.
36. Zhang Y, Wei Y, Jiang B, Chen L, Bai H, Zhu X, et al. Scavenger receptor A1 prevents metastasis of non-small cell lung cancer *via* suppression of macrophage serum amyloid A1. *Cancer Res* 2017;**77**:1586−98.
37. Pascual-García M, Bonfill-Teixidor E, Planas-Rigol E, Rubio-Perez C, Iurlaro R, Arias A, et al. LIF regulates CXCL9 in tumor-associated macrophages and prevents $CD8^+$ T cell tumor-infiltration impairing anti-PD1 therapy. *Nat Commun* 2019;**10**:2416.
38. Li AD, Xie XL, Qi W, Wang WB, Ma JJ, Zhao DQ, et al. TGR5 promotes cholangiocarcinoma by interacting with mortalin. *Exp Cell Res* 2020;**389**:111855.
39. Yang JI, Yoon JH, Myung SJ, Gwak GY, Kim W, Chung GE, et al. Bile acid-induced TGR5-dependent c-Jun-N terminal kinase activation leads to enhanced caspase 8 activation in hepatocytes. *Biochem Biophys Res Commun* 2007;**361**:156−61.
40. Xiong Q, Huang H, Wang N, Chen R, Chen N, Han H, et al. Metabolite-sensing G protein coupled receptor TGR5 protects host from viral infection through amplifying type I interferon responses. *Front Immunol* 2018;**9**:2289.
41. Yanguas-Casás N, Barreda-Manso MA, Nieto-Sampedro M, Romero-Ramírez L. TUDCA: an agonist of the bile acid receptor GPBAR1/TGR5 with anti-inflammatory effects in microglial cells. *J Cell Physiol* 2017;**232**:2231−45.
42. Sunahara RK, Taussig R. Isoforms of mammalian adenylyl cyclase: multiplicities of signaling. *Mol Interv* 2002;**2**:168−84.
43. Guo C, Xie S, Chi Z, Zhang J, Liu Y, Zhang L, et al. Bile acids control inflammation and metabolic disorder through inhibition of NLRP3 inflammasome. *Immunity* 2016;**45**:802−16.
44. Fu C, Jiang L, Hao S, Liu Z, Ding S, Zhang W, et al. Activation of the IL-4/STAT6 signaling pathway promotes lung cancer progression by increasing M2 myeloid cells. *Front Immunol* 2019;**10**:2638.
45. Qin J, Zhang X, Tan B, Zhang S, Yin C, Xue Q, et al. Blocking P2X7-mediated macrophage polarization overcomes treatment resistance in lung cancer. *Cancer Immunol Res* 2020;**8**:1426−39.
46. Zhang X, Zeng Y, Qu Q, Zhu J, Liu Z, Ning W, et al. PD-L1 induced by IFN-γ from tumor-associated macrophages *via* the JAK/STAT3 and PI3K/AKT signaling pathways promoted progression of lung cancer. *Int J Clin Oncol* 2017;**22**:1026−33.
47. Lu C, Talukder A, Savage NM, Singh N, Liu K. JAK-STAT-mediated chronic inflammation impairs cytotoxic T lymphocyte activation to decrease anti-PD-1 immunotherapy efficacy in pancreatic cancer. *OncoImmunology* 2017;**6**:e1291106.
48. Bremnes RM, Busund LT, Kilvær TL, Andersen S, Richardsen E, Paulsen EE, et al. The role of tumor-infiltrating lymphocytes in development, progression, and prognosis of non-small cell lung cancer. *J Thorac Oncol* 2016;**11**:789−800.